Materials Physics and Mechanics 42 (2019) 103-111 Received: October 6, 2018

THE TIME-STEP BOUNDARY-ELEMENT SCHEME ON THE NODES OF THE LOBATTO METHOD IN PROBLEMS OF 3-D DYNAMIC POROELASTICITY

L.A. Igumnov[1], A.N. Petrov[2]*, I.V. Vorobtsov[1]

[1]Research Institute for Mechanics, National Research Lobachevski State University of Nizhniy Novgorod, 23, Gagarin Ave., bld. 6, Nizhniy Novgorod, 603950, Russia

[2]Research and Education Center "Materials", Don State Technical University, 1, Gagarin Sq., Rostov-on-Don, 344010, Russia

*e-mail: andrey.petrov@mech.unn.ru

Abstract. A boundary-element scheme for analyzing initial boundary-value problems of 3-D porelasticity is considered. The scheme is based on a time-step method of numerically inverting Laplace transform. According to the method, a solution in time is calculated using quadrature formulas, based on complex values of the function in specific points. The choice of the points is determined by Lobatto method being one of Runge-Kutta methods. A possibility of using two- and three-stage Lobatto methods is considered. Using as an example the problem about a force, acting upon end of a prismatic poroelastic body, the effect of time-step on the dynamic responses of the forces is studied. The present results are compared with the results obtained on the nodes of Radau method.

Keywords: boundary element method, Runge-Kutta method, poroelasticity, transient dynamic analysis, wave propagation

1. Introduction

Studying wave propagation in poroelastic bodies subjected to dynamic loading is important in many engineering applications. The results of such studies are used to develop methods of non-destructive check, in soil structure analysis and earthquake seismology. Very often, an analytical solution to wave propagation problems is only possible in some special cases and for particular kinds of boundary conditions, so that numerical approximation methods such as the boundary element method (BEM) have been used. The BEM is especially suitable for wave propagation problems since it requires the formulation of the problem only along the boundary and produces highly accurate solutions.

In BEM-modeling of dynamic processes, three main approaches can be conventionally discerned: solving in time domain [1], solving in Laplace or Fourier transforms with the subsequent inversion of the transforms [2], and the dual reciprocity approach [3]. The numerical accuracy of the time-domain BEM with time-stepping discretization is strongly influenced by the time step size. In particular, the time-marching process becomes numerically unstable when using collocation methods, where the time step size is smaller than the element size. To overcome this difficulty, a number of stabilization techniques were developed [4, 5]. However, the time-domain approach cannot be used to solve wave propagation problems for poroelastic media due to the absence of fundamental solutions in time. Methods working in the frequency domain also have their limitations, as they require

http://dx.doi.org/10.18720/MPM.4212019_9

efficient numerical techniques for inverse transforms and are applicable only to problems for which the correspondence principle is valid.

In 1988, Lubich [6,7] introduced the convolution quadrature method (CQM) to discretize the convolution integral. It gained significant interest as a technique (CQ-BEM) for applying the BEM to time-dependent problems where classical time-step schemes suffer from instability and numerical damping [8 – 10]. Later, it was shown in several studies that the CQ-BEM based on implicit Runge–Kutta method provides better accuracy than that based on the linear multistep method [11–15]. Moreover, Banjai and Sauter reformulated CQ-BEM approach to solve decoupled problems in Laplace domain that works as a transformation method [16]. Retaining the numerical stability properties of the original method, this approach has the time step size as the only parameter determined by the physical parameters of the problem. The applicability of the reformulated CQ-BEM to solution of poroelastic problems was demonstrated by Schanz, but only using the linear multistep method [17].

This study presents a modification of such a time-step scheme on the nodes of Runge-Kutta methods, exemplified by 2- and 3-stage Lobatto method. The time-step BEM scheme is based on the stepped method for numerically inverting Laplace transforms. This method is similar in its formulation to the CQM, but in contrast to it is based on the theorem of operational calculus for integrating in time-domain. The application of the scheme to problems of wave propagation in partially saturated media is considered.

2. Governing differential equations

To describe a poroelastic continuum, Biot's mathematical model of a material is used, in which (the material) a solid phase, representing a form-generating skeleton, carrying the main stress load, and two fluid phases – water and air filling the pore system, are discerned. All the three phases are assumed compressible. Temperature variations are neglected. Moreover, porosity φ and saturation degree of the material S_f are defined as:

$$\varphi = \frac{V_{void}}{V}, S_f = \frac{V_f}{V_{void}}, \tag{1}$$

where V_{void} is the volume of interconnected pores in the specimen, V is the total volume of the material, V_f is the volume of the filler, and it is assumed that $f = a$ for air and $f = w$ for water. Consider a case where the pores are completely filled:

$$S_a + S_w = 1. \tag{2}$$

The bulk density is defined as

$$\rho = (1-\varphi)\rho_s + \varphi S_w \rho_w + \varphi S_a \rho_a, \tag{3}$$

where the densities of the solid, water and air is denoted by $\rho_s, \rho_w\ \rho_a$, respectively.

In order to describe mechanical behavior of the partially saturated porous medium, the effective stress principle is used, which was introduced by Terzaghi [18]. The corresponding defining relations in terms of stress are expressed similarly to that adopted for fully saturated conditions [19, 20]:

$$\sigma'_{ij} = \sigma_{ij} + \alpha(S_a p_a - S_w p_w)\delta_{ij}, \tag{4}$$

where σ'_{ij} is the effective stress, σ_{ij} is the total stress, p_a denotes the pore air pressure, p_w is the pore water pressure, α is a Biot constant. The coefficient α is described by the relationship:

$$\alpha = 1 - \frac{K}{K_s}, \tag{5}$$

where K is the bulk modulus of the solid skeleton and K_s is the bulk modulus of the solid grains.

The solid skeleton is assumed elastic isotropic. Due to this fact, the effective stress tensor is given by

$$\sigma'_{ij} = \left(K - \frac{2}{3} G \right) \varepsilon_{kk} \delta_{ij} + 2G\varepsilon_{ij}, \tag{6}$$

where G denotes the shear modulus, ε_{ij} denotes the strain tensor. The components of strain tensor ε_{ij} of a solid and displacements u_i are mutually coupled by the geometric relations:

$$\varepsilon_{ij} = \frac{1}{2}\left(u_{i,j} + u_{j,i} \right). \tag{7}$$

To construct equations of motion, defining equations must be combined with the related balance equations of momentum and balance equations of mass for each of the phases (for details see [21]). Using a Laplace transform makes it possible to write down the dynamic equations of a poroelastic medium in the form of a boundary-value problem for unknown displacement functions of the elastic skeleton $\hat{u}_i$ and the pore pressures of the fillers $\hat{p}^w$ and $\hat{p}^a$:

$$\begin{bmatrix} B_1\delta_{ij} + B_2\partial_i\partial_j & B_3\partial_i & B_4\partial_i \\ B_5\partial_j & B_6 & B_7 \\ B_8\partial_j & B_9 & B_{10} \end{bmatrix} \begin{bmatrix} \hat{u}_i \\ \hat{p}^w \\ \hat{p}^a \end{bmatrix} = \begin{bmatrix} -\hat{F}_i \\ -\hat{I}^w \\ -\hat{I}^a \end{bmatrix}, \tag{8}$$

here

$$B_1 = G\nabla^2 - (\rho - \beta S_w \rho_w - \gamma S_a \rho_a)s^2,\ B_2 = K + \frac{G}{3},\ B_3 = -(\alpha - \beta)S_w, \tag{9}$$

$$B_4 = -(\alpha - \gamma)S_a,\ B_5 = -(\alpha - \beta)S_w s,\ B_6 = -\left(\zeta S_{ww} S_w + \frac{\varphi}{K_w} S_w - S_u \right) s + \frac{\beta S_w}{\rho_w s}\nabla^2, \tag{10}$$

$$B_7 = -\left(\zeta S_{aa} S_w + S_u \right) s,\ B_8 = -\left(\alpha - \gamma \right) S_a s\ B_9 = -\left(\zeta S_{ww} S_a + S_u \right) s, \tag{11}$$

$$B_{10} = -\left(\zeta S_{aa} S_a + \frac{\varphi}{K_a} S_a - S_u \right) s + \frac{\gamma S_a}{\rho_a s}\nabla^2, \tag{12}$$

where K_w and K_a are bulk moduli of the fluid, $\hat{F}_i$, $\hat{I}^w$, $\hat{I}^a$ are bulk body forces. Symbol "^" denotes Laplace transform with complex variable s.

The following abbreviations:

$$\zeta = \frac{\alpha - \varphi}{K_s},\ S_{ww} = S_w - \vartheta(S_w - S_{rw}),\ S_{aa} = S_a + \vartheta(S_w - S_{rw}), \tag{13}$$

$$S_u = -\frac{\vartheta(S_{ra} - S_{rw})}{p^d}\left(\frac{S_w - S_{rw}}{S_{ra} - S_{rw}} \right)^{\frac{\vartheta+1}{\vartheta}}, \tag{14}$$

are introduced, where S_{rw} is the residual wetting fluid saturation and S_{ra} is the non-wetting fluid entry saturation. The symbol p^d is the non-wetting fluid entry pressure, ϑ is the pore size distribution index. For most rocks, ϑ falls between 0.4 and 4. The symbols β and γ are Laplace parameter dependent variables and expressed as

$$\beta = \frac{\kappa_w \varphi \rho_w s}{\varphi S_w + \kappa_w \rho_w s},\ \gamma = \frac{\kappa_a \varphi \rho_a s}{\varphi S_a + \kappa_a \rho_a s}, \tag{15}$$

where κ_w and κ_a the phase permeability of the wetting and the non-wetting fluid are given by $\kappa_w = K_{rw}k/\eta_w$ and $\kappa_a = K_{ra}k/\eta_a$, respectively. K_{rw} and K_{rw} denotes the relative fluid phase permeability, k denotes the intrinsic fluid permeability, η_w and η_a are viscosity of the fluid. To evaluate relative phase permeability the following equations are used:

$$K_{rw} = S_e^{(2+3\vartheta)/\vartheta},\ K_{ra} = (1-S_e)^2\left(1-S_e^{(2+\vartheta)/\vartheta}\right), \tag{16}$$

where S_e denotes the effective wetting fluid saturation degree given by

$$S_e = \frac{S_w - S_{rw}}{S_{ra} - S_{rw}}. \tag{17}$$

3. Laplace transform inversion

The stepped method for numerically inverting Laplace transforms is described in this section in brief. This method is close in its formulation to the CQM, but, in contrast to it, is based on the operational calculus of integrating original $f(s)$ of representation $\hat{f}(s)$. In general, the integral

$$y(t) = \int_0^t f(\tau)d\tau \tag{18}$$

is approximated as follows [22]:

$$y(0) = 0,\ y(n\Delta t) = \mathbf{b}^T\mathbf{A}^{-1}\sum_{k=1}^{n}\boldsymbol{\omega}_k^{\Delta t}, n = 1,...N, \tag{19}$$

where *N* is the number of equal time steps. In this expression, the quadrature weights $\boldsymbol{\omega}_k^{\Delta t}$ are determined using Laplace representation $\hat{f}(s)$ and the Runge-Kutta method. The quadrature weights can be expressed by Cauchy integral form and approximated by using a trapezoidal rule with the number of steps *L* as follows:

$$\boldsymbol{\omega}_n^{\Delta t} = \frac{R^{-n}}{L}\sum_{l=0}^{L-1}\hat{f}\left(\frac{\psi(z)}{\Delta t}\right)\frac{\psi(z)}{\Delta t}e^{-nl\frac{2\pi}{L}\mathrm{i}},\ z = Re^{l\frac{2\pi}{L}\mathrm{i}}, \tag{20}$$

$$\psi(z) = \mathbf{A}^{-1} - z\mathbf{A}^{-1}\mathbf{1}\mathbf{b}^T\mathbf{A}^{-1}, \tag{21}$$

where $\psi(z)$ is characteristic function of the Runge-Kutta method and $\mathbf{1} = (1,1,...,1)^T$. The parameter *R* can be calculated by

$$R^L = \sqrt{\varepsilon}, \tag{22}$$

where ε is the error of the numerical calculation of Equation (20).

The approximation used in deriving formulas (20), (21) is based on using the *m*-stage Runge-Kutta method written down using Butcher's table:

$$\frac{\mathbf{c}\,|\,\mathbf{A}}{\mathbf{b}^T},\ \mathbf{A}\in\mathbb{R}^{m\times m},\ \mathbf{b},\mathbf{c}\in\mathbb{R}^m. \tag{23}$$

A correct formulation of a time-step scheme requires that the method be A-stable and L-stable. In the assumption of $\mathbf{b}^T\mathbf{A}^{-1} = (0,...,0,1)$, the method is automatically L-stable. It is also important to note that the quadrature weights $\boldsymbol{\omega}_k^{\Delta t}$ and the characteristic function $\psi(z)$ are *m*-order matrices.

In the present study, Lobatto (Lobatto IIIC) and Radau (Radau IIA) schemes were chosen as a particular example of the Runge-Kutta schemes meeting the formulated conditions.

4. BEM formulation and numerical procedure

The boundary-element technique is based on the use of a regularized BIE direct approach [23]:

$$\int_{\Gamma}\left(\mathbf{T}(\mathbf{x},\mathbf{y},s)\mathbf{u}(\mathbf{x},s)-\mathbf{T}^{\mathbf{0}}(\mathbf{x},\mathbf{y})\mathbf{u}(\mathbf{y},s)\right)d\Gamma=\int_{\Gamma}\mathbf{U}(\mathbf{x},\mathbf{y},s)\mathbf{t}(\mathbf{x},s)d\Gamma,\ \mathbf{x},\mathbf{y}\in\Gamma,\Gamma=\partial\Omega, \tag{24}$$

where $\mathbf{U}(\mathbf{x},\mathbf{y},s)$ and $\mathbf{T}(\mathbf{x},\mathbf{y},s)$ are matrices of fundamental and singular solutions, respectively [24], $\mathbf{T^0}(\mathbf{x},\mathbf{y})$ contains isolated singularities, **x** is the integration point, **y** is the observation point, **u** is the generalized displacement vector, **t** is the generalized force vector.

To solve Equation (24), the boundary surface Γ is divided into generalized eight-node quadrangular elements; the coordinates of the points on the *k* element are determined from the relation:

$$\mathbf{x}(\xi)=\sum_{m=1}^{8}N_m(\xi)\mathbf{x}_m^k, \tag{25}$$

where N_m are bilinear shape functions, $\xi=(\xi_1,\xi_2)\in[-1,1]^2$ are local coordinates, $\mathbf{x}_m^k$ are global coordinates of nodes [25].

Generalized boundary functions of the first kind are approximated bi-linearly, and generalized boundary functions of the second kind are assumed constant over the element:

$$\mathbf{u}(\xi)=\sum_{l=1}^{4}R_l(\xi)\mathbf{u}_l^k,\ \mathbf{t}(\xi)=\mathbf{t}^k, \tag{26}$$

where $R_l(\xi)$ are the bilinear shape functions, $\mathbf{u}_l^k$ and $\mathbf{t}^k$ are the values of generalized functions in the nodes of the *k*-th element.

The discrete representation of BIE (24) is constructed at the interpolation nodes of unknown boundary functions (collocation points) and has the following matrix form:

$$[\Delta\mathbf{G}]\{\mathbf{T}\}=[\Delta\mathbf{F}]\{\mathbf{U}\}. \tag{27}$$

Matrices $\Delta\mathbf{G}$ and $\Delta\mathbf{F}$ contain integrals of the components of matrices $\mathbf{U}(\mathbf{x},\mathbf{y},s)$ and $\mathbf{T}(\mathbf{x},\mathbf{y},s)$, multiplied by the form functions. The choice of the numerical integration scheme for computing the integral depends on its type. When a collocation point lies on integration element, the procedure for revealing the feature is performed. To improve the accuracy of integration on an element that does not contain a collocation point, in addition to the Gauss integration formulas, a hierarchical integration algorithm is applied, wherein the element is subdivided until the specified accuracy is achieved.

5. Numerical results

The 3D poroelastic column loaded by a Heaviside function is investigated as example to study the behavior of transformation method. The width of the column is $b = 1$ m, the height $h = 3$m. The column has zero displacements on one end and the normal force $t_3=-1N/m^2$ on the other end is prescribed. A boundary-element discretization consisting of 896 quadrangular elements is used in the computations. The sketch of problem is shown in Fig. 1. The parameters of the partially saturated porous material correspond to those of sandstone: $\varphi=0.23$, $\rho_s=2650kg/m^3$, $\rho_w=997kg/m^3$, $\rho_a=1.01kg/m^3$, $K=1,02\times10^9Pa$, $G=1.44\times10^9Pa$, $K_s=3.5\times10^{10}Pa$, $K_w=2.25\times10^9Pa$, $K_a=1.1\times10^5Pa$, $k=2.5\times10^{-12}m^2$, $\mu_w=1.0\times10^{-3}N\cdot s/m^2$, $\mu_a=1.8\times10^{-5}N\cdot s/m^2$.

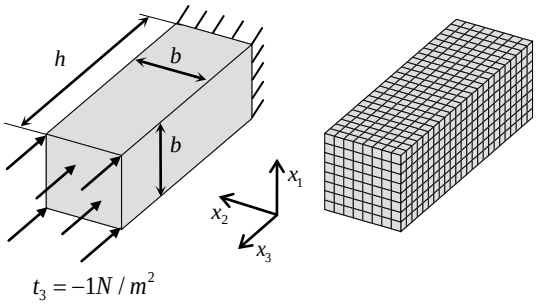

Fig. 1. Geometry and boundary conditions of a partially saturated poroelastic column

The boundary-element solutions obtained using different methods of the Runge-Kutta family are compared for the values of forces t_3 in the rigidly fixed part of the column. Jumping change of the forces makes it possible to compare the results in the conditions of additional difficulties of approximation. The boundary-element solutions are also compared with a one-dimensional numerical-analytical solution. Time step Δt is taken to be 0.00005 *s* for the 2-stage methods, and 0.0002 *s* for the 3-stage ones. The total number of complex-valued points required for computing a solution is assumed constant for all the methods. The diagrams of forces are present in Figs. 2 – 5.

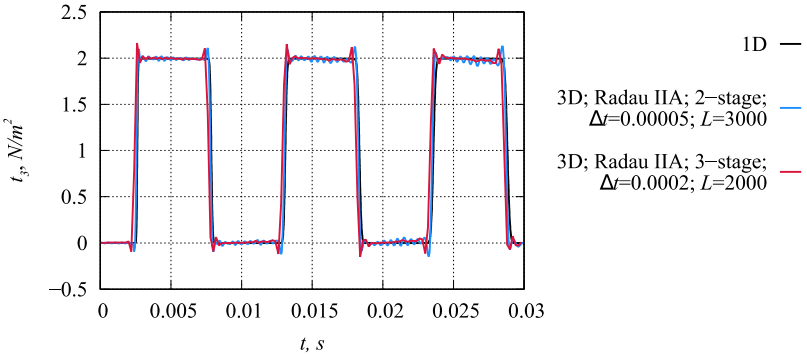

Fig. 2. Force solution t_3 at the fixed end versus time for the 2- and 3-stage Radau IIA method

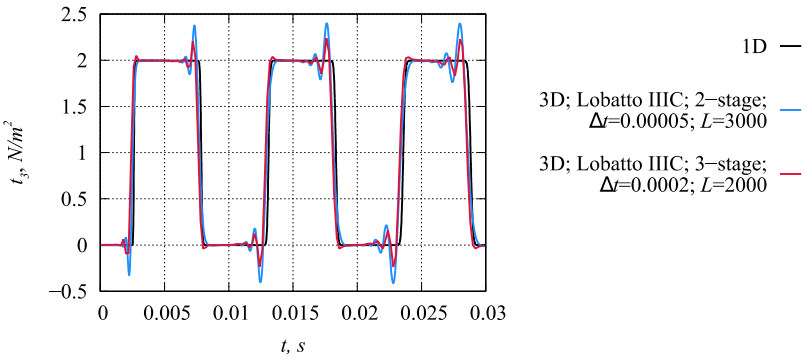

Fig. 3. Force solution t_3 at the fixed end versus time for the 2- and 3-stage Lobatto IIIC method

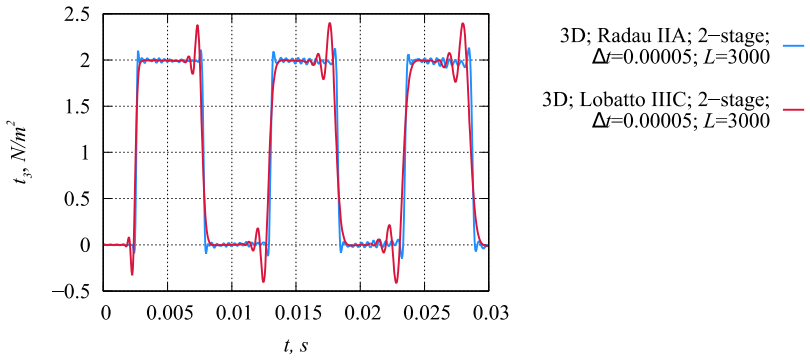

Fig. 4. Force solution t_3 at the fixed end versus time for the 2-stage Lobatto IIIC method compared to the solution for the 2-stage Radau IIA method

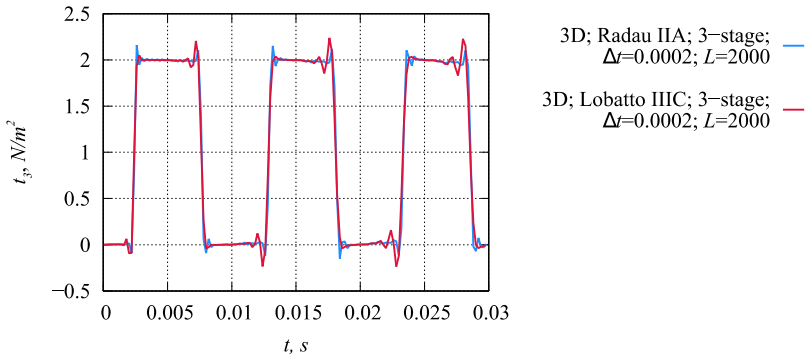

Fig. 5. Force solution t_3 at the fixed end versus time for the 3-stage Lobatto IIIC method compared to the solution for the 3-stage Radau IIA method

It is evident in Figs. 2, 3 that the boundary-element solutions obtained at the nodes of the Lobatto and Radau methods are close to the numerical-analytical solution of the one-dimensional problem. The 2- and 3-stage Radau methods in problems of boundary-element modeling of the dynamics of fully saturated poroelastic bodies are compared in [12] for the values of flow. The present study corroborates the conclusions made in [12] and makes it possible to extend them to include the case of using 2- and 3-stage Lobatto methods in problems of boundary-element modeling of the dynamics of partially saturated poroelastic bodies. In particular, it can be observed (Figs. 2, 3) that the forces computed using the 3-stage versions of the both Runge-Kutta methods have smaller perturbation amplitude at the jump points. Moreover, the propagation interval of the oscillations is also smaller than the range in the case of using the 2-stage versions. Though in the first case, a long time step is used due to the sensibility of the 3-stage methods to small steps, the force curve is quite smooth. Separate comparison of the 2-stage methods reveals that Radau method yields forces of considerably smaller perturbation amplitude in the jump points and of considerably smaller propagation interval (Fig. 4). In this case, minor oscillations of the forces over the entire time interval are also observed, testifying to the closeness of the time step chosen to its maximal value. At the same time, the forces obtained using the 2-stage Lobatto method do not show any oscillations of this kind. Similar effects, but less pronounced, are observed, when comparing the 3-stage methods (Fig. 5). Based on the conducted investigations, it can be asserted that the use of 3-stage methods of the Runge-Kutta family proves more preferable in the case of step change of the solution.

6. Conclusion

A boundary-element scheme on the nodes of 2- and 3-stage Lobatto methods for analyzing dynamic problems of partially saturated poroelastic bodies is present. A mathematical model of a partially saturated poroelastic medium is given. Results of the numerical analyses are present, which corroborate the conclusions of other authors concerning the combined use of BEM and methods of the Runge-Kutta family. The conclusions are extended to include the use 2- and 3-stage Lobatto methods in problems of boundary-element modeling of the dynamics of partially saturated poroelastic bodies.

Acknowledgements. *The research was carried out under the financial support of the Russian Science Foundation (project No. 15-19-10056).*

References

[1] Mansur WJ. *A Time-Stepping Technique to Solve Wave Propagation Problems Using the Boundary Element Method*. Southampton: University of Southampton; 1983.
[2] Cruse TA, Rizzo FJ. A direct formulation and numerical solution of the general transient elastodynamic problem. I. *Journal of Mathematical Analysis and Applications*. 1968;22: 244-259.
[3] Aliabadi MH. *The Boundary Element Method: Applications in Solids and Structures*. London: Wiley; 2002.
[4] Guoyou Y, Mansur WJ, Carrer JAM, Gong L. Stability of Galerkin and collocation time domain boundary element methods as applied to the scalar wave equation. *Computers & Structures*. 2000;74(4): 495-506.
[5] Ha-Duong T, Ludwig B, Terrasse I. A Galerkin BEM for transient acoustic scattering by an absorbing obstacle. *International Journal for Numerical Methods in Engineering*. 2003;57(13): 1845-1882.
[6] Lubich C. Convolution quadrature and discretized operational calculus I. *Numerische Mathematik*. 1988;52(2): 129-145.
[7] Lubich C. Convolution quadrature and discretized operational calculus II. *Numerische Mathematik*. 1988;52(4): 413-425.
[8] Schanz M, Antes H. Application of 'Operational Quadrature Methods' in time domain boundary element method. *Meccanica*. 1997;32(3): 179-186.
[9] Abreu AI, Carrer JAM, Mansur WJ. Scalar wave propagation in 2D: a BEM formulation based on the operational quadrature method. *Engineering Analysis with Boundary Elements*. 2003;27(2): 101-105.
[10] Zhang Ch. Transient elastodynamic antiplane crack analysis of anisotropic solids. *International Journal of Solids and Structures*. 2000;37(42): 6107-6130.
[11] Lubich CH, Ostermann A. Runge-Kutta methods for parabolic equations and convolution quadrature. *Mathematics of Computation*. 1993;60(201): 105-131.
[12] Banjai L, Messner M, Schanz M. Runge-Kutta convolution quadrature for the Boundary Element Method. *Computer Methods in Applied Mechanics and Engineering*. 2012;245-246: 90-101.
[13] Calvo MP, Cuesta E, Palencia C. Runge-Kutta convolution quadrature methods for well-posed equations with memory. *Numerische Mathematik*. 2007;107(4): 589-614.
[14] Banjai L, Lubich C. An error analysis of Runge–Kutta convolution quadrature. *BIT Numerical Mathematics*. 2011;51(3): 483-496.
[15] Banjai L, Lubich C, Melenk JM. Runge-Kutta convolution quadrature for operators arising in wave propagation. *Numerische Mathematik*. 2011;119(1): 1-20.
[16] Banjai L, Sauter S. Rapid solution of the wave equation in unbounded domains. *SIAM Journal on Numerical Analysis*. 2008;47(1): 227-249.

[17] Schanz M. On a reformulated convolution quadrature based boundary element method *Computer Modeling in Engineering & Sciences*. 2010;58(2): 109-128.
[18] Terzaghi K. *Theoretical Soil Mechanics*. New York: John Wiley and Sons; 1943.
[19] Bishop AW. The principle of effective stress. *Teknisk Ukeblad*. 1959;106(39): 859-863.
[20] Bishop AW, Eldin AKG. Undrained triaxial tests on saturated sands and their significance in the general theory of shear strength. *Geotechnique*. 1950;2(1): 13-32.
[21] Li P, Schanz M. Time domain boundary element formulation for partially saturated poroelasticity. *Engineering Analysis with Boundary Elements*. 2013;37(11): 1483-1498.
[22] Igumnov L, Ipatov A, Belov A, Petrov A. A combined application of boundary-element and Runge-Kutta methods in three-dimensional elasticity and poroelasticity. *EPJ Web of Conferences*. 2015;94: 04026.
[23] Bazhenov VG, Igumnov LA, *Boundary Integral Equations and Boundary Element Methods in Treating the Problems of 3D Elastodynamics with Coupled Fields*. Moscow: PhysMathLit; 2008.
[24] Amenitsky AV, Belov AA, Igumnov LA, Karelin IS. Boundary integral equations for analyzing dynamic problems of 3-D porouselasticity. *Problems of Strength and Plasticity*. 2009;71:164-171.
[25] Igumnov LA, Litvinchuk SY, Petrov AN, Ipatov AA. Numerically analytical modeling the dynamics of a prismatic body of two- and three-component materials. In: Parinov IA, Chang SH, Topolov VY. (eds.) *Advanced Materials. Springer Proceedings in Physics*. Springer Proceedings in Physics book series (SPPHY, vol. 175). Cham: Springer; 2016. p.505-516.